29th International Congress on Sound and Vibration
The annual congress of the International Institute of Acoustics and Vibration (IIAV)
9–13 July 2023
ICSV29

ON THE SENSITIVITY ANALYSIS OF THREE-PORT MEASUREMENTS FOR ACOUSTIC CHARACTERISATION OF PERFORATES

Shail A. Shah, Hans Bodén, and Susann Boij
KTH Royal Institute of Technology, Stockholm, Sweden
email: shail@kth.se

Perforates, often with a backing cavity, are used in noise reducing liners and silencers for aircraft engines and internal combustion engines. Direct methods of impedance estimation can be used for the acoustic characterisation of the perforated plates standalone, without the backing cavity, in presence of grazing flow. The three-port technique is a direct method for estimating the transfer impedance of perforates in presence of grazing flow and high-amplitude acoustic excitation. In a previous study, the dependence of the experimentally determined transfer impedance on the operating conditions, namely the in-duct temperature, the grazing flow speed and microphone distances is shown. This paper is a follow up to the previous study and attempts to quantify the effect of variations in these testing conditions on the real part of the transfer impedance, i.e., the resistance. The possible sources of errors and deviations in the determination of the operating conditions are discussed. Based on the uncertainty range of the operating conditions, a Monte-Carlo simulation is performed to calculate the confidence intervals of the results. Additionally, the effect of the error distribution on the confidence intervals is displayed.

Keywords: perforates, impedance, error analysis, Monte-Carlo analysis, grazing flow

1. Introduction

Perforated plates are installed in ducts to attenuate the propagating sound using thermo-viscous dissipation, e.g., nacelle liners in aircraft engine. The standard operating conditions considered for designing a liner are the presence of grazing flow and high-amplitude acoustic excitation [1]. Characterisation of the passive acoustic behaviour of the perforate is carried out using the transfer impedance. The real part of the transfer impedance, i.e., the resistance, represents the acoustic attenuation caused by the presence of the perforate. Direct methods of impedance estimation are used to experimentally characterise the perforate [2, 3]. An example of a direct method is the three-port measurement technique [4, 5], used in this study. The perforate sample is examined in the presence of grazing flow and acoustic excitation from three-different directions.

A previous study shows that the experimentally determined resistance using the three-port technique is susceptible to errors in the determination of the testing conditions, namely the in-duct temperature, the grazing flow speed, and the microphone distances [6].

An error analysis, based on Monte-Carlo simulation can be used to quantify the effect of these errors on the results. The error distribution of the inputs affects the standard deviation of the Monte-Carlo outputs. Hence, it is necessary to use the correct distribution type of the inputs, as discussed in Section 3. In Section 4, the results of the Monte-Carlo simulation are discussed. A preliminary observation suggests that the uncertainty in the resistance is weakly dependent on the uncertainty in the grazing flow speed. However, to further study the individual dependence of each input factor, a global sensitivity analysis is necessary.

2. Experimental Technique

The three-port measurement technique for the acoustic characterisation of a perforate includes of a perforate flush-mounted at the intersection of the rectangular T-Junction, as shown in Fig. 1 [5]. The configuration allows the perforate to be studied under plane-wave acoustic excitation from three different directions and in presence of grazing flow.

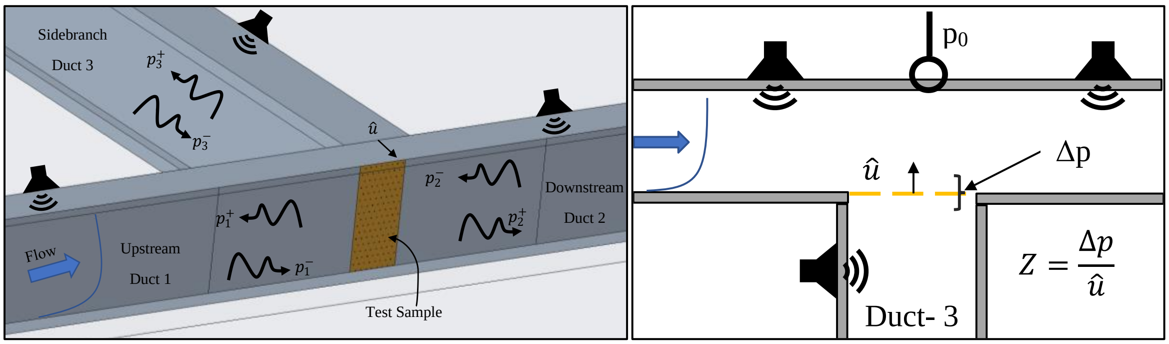

Figure 1 a) 3-D Sketch of the three-port setup; b) Calculation of the transfer impedance of the perforate

Data acquisition of the acoustic pressure was carried out using three flush-mounted calibrated microphones in each duct. Using the acquired pressure data, and the distance (s) between the microphones and the acoustic origin of the three-port as inputs, the multi-microphone method [5] is incorporated to perform wave decomposition. The multi-microphone method assumes hard-wall acoustic boundary conditions and plane-wave propagation between the microphones. Hence the decomposed amplitudes are also a function of the complex wavenumber (k), and by extension the in-duct temperature (T) and the grazing flow speed (U). The sound pressure level in the duct was maintained to be $<$ 110 dB. Hence, a linear regime can be assumed.

To minimise errors due to random noise, the frequency response function (p) between the measured acoustic pressure and the voltage of the exciting loudspeaker was used for post-processing. The sources of errors in the multi-microphone method hence include the properties of $T, U, p,$ and s.

Following the wave decomposition, the three-port scattering matrix ($\boldsymbol{S}$) was determined [7], as shown in Eq. (1)

$$\begin{bmatrix} p_{1+} \\ p_{2+} \\ p_{3+} \end{bmatrix} = \begin{bmatrix} r_1 & \tau_{2\to1} & \tau_{3\to1} \\ \tau_{1\to2} & r_2 & \tau_{3\to2} \\ \tau_{1\to3} & \tau_{2\to3} & r_3 \end{bmatrix} \begin{bmatrix} p_{1-} \\ p_{2-} \\ p_{3-} \end{bmatrix}, or\ p^+ = \boldsymbol{S}\boldsymbol{p}^-, \quad (1)$$

where $p_{x\pm}$ are the results of wave decomposition, and $r_x, \tau_{x\to y}$ represent the reflection and transmission coefficients of $\boldsymbol{S}$, respectively.

The calculation of the normalised transfer impedance ($\overline{Z}$) using the coefficients of $\boldsymbol{S}$ is shown in [4], and follows Eq. (2). The passive-acoustic characteristic of interest in this study is the real part $\overline{Z}$, i.e., the resistance (R).

$$\overline{Z_1} = \frac{(r_1 + \tau_{1\to2} + 1)}{2\tau_{1\to3}} - 1 \quad (2)$$

$$\overline{Z_2} = \frac{(r_2 + \tau_{2\to1} + 1)}{2\tau_{2\to3}} - 1$$
$$\overline{Z_3} = \frac{1 + r_3}{1 - r_3} - \frac{1}{2}\left(\frac{\tau_{3\to1} + \tau_{3\to2}}{1 - \rho_3}\right),$$

where $\overline{Z_x}$ is the normalised transfer impedance calculated under acoustic excitation from duct – x.
The measurement equipment and the technique is explained in further detail in [5].

3. Uncertainty Quantification

To quantify the effect of the errors in the inputs ($T, U, p,$ and s) on the output (R) a Monte-Carlo simulation was carried out. Using the results of the Monte-Carlo simulation, the mean (μ), and the variance (σ) of R is determined and the 95% confidence intervals (CI) are calculated.

The first subsection discusses the considered uncertainty range and the distribution of each inputs. The following subsection 3.2 discusses the calculation of the Monte-Carlo simulation.

3.1 Error distribution of Inputs

The sources of error in the determination of the inputs to the multi-microphone method include instrumentation error and reading error [8]. The propagation of the uncertainty from the sensor to the value used for post-processing is calculated following the method explained in [8]. Using the measured value as the mean, the uncertainty range for each input, as well as its distribution was defined as following:

- **Temperature**: The in-duct temperature was measured using a calibrated and flush-mounted K-type thermocouple. The uncertainty range in temperature used for post-processing was calculated using the deviation in the measured static temperature over the course of the acoustic measurement, and the standard error range of the data acquisition system [9]. The distribution of the error is hence assumed to be random in nature. The uncertainty range was found to be within ± 1.5 K.
- **Grazing flow speed**: The bulk speed of the grazing flow was calculated as the integral average of the flow profile measured using a pitot-tube. The deviation in the bulk speed when measured across the two cross-section dimensions of the duct approximates 7% of the bulk speed [6]. This suggests a 7% uncertainty in the 2-D flow profile of the duct. Moreover, in [5], it is shown that the bulk speed can be calculated by scaling the maximum speed measured, i.e., at the centre of the cross-section. The scaling ratio is linearly dependent on the grazing flow speed and is, by extension, another source of uncertainty. Lastly, the standard error of the flow meter [10] also needs to be accounted to calculate the uncertainty range of the determined grazing flow bulk speed. The propagation of uncertainty was calculated, and it was found that the error in the estimation of the 2-D flow profile dominates. As this approximates a normal distribution curve, the uncertainty distribution for the flow speed was assumed to be of a normally distributed type. In the flow speed range of the measurements ($\approx 10\ \mathrm{m.s^{-1}} < U < \approx 60\ \mathrm{m.s^{-1}}$), the uncertainty was determined to be < 5 $\mathrm{m.s^{-1}}$.
- **Microphone distances**: In this study, the uncertainty in the determination of the geometric distance between the centre of the microphone and the acoustic origin of the three-port was considered to be due to a reading error. The range is arbitrarily chosen to be ± 1 mm, and a normal distribution of the uncertainty is assumed.
- **Sound field determination:** The frequency response function between the microphone signal and the loudspeaker voltage is used for determining the acoustic field in the three-port. In [8] it is shown that in presence of grazing flow, the most significant factor while calculating uncertainty in the measured frequency response function is the signal-to-noise ratio (SNR). Across the frequency

range of the measurements, the minimum value of the SNR is used to determine the uncertainty range of the frequency response functions. As the uncertainty is due to the presence of flow noise, its distribution is assumed to be of a random type. The minimum value of the SNR (≈13 dB) was observed at the grazing flow speed of $U \approx 60\ \mathrm{m.s^{-1}}$ and at 2250 Hz.

Within these uncertainty ranges, 10000 samples were chosen to be used as inputs for the Monte-Carlo simulation. In case of the input distribution of random type, Sobol sequencing [11] was used to choose the input points within the error range. An example of such distribution is shown in Fig. 2 which displays the uncertainties in the measured in-duct temperature at different grazing flow speeds.

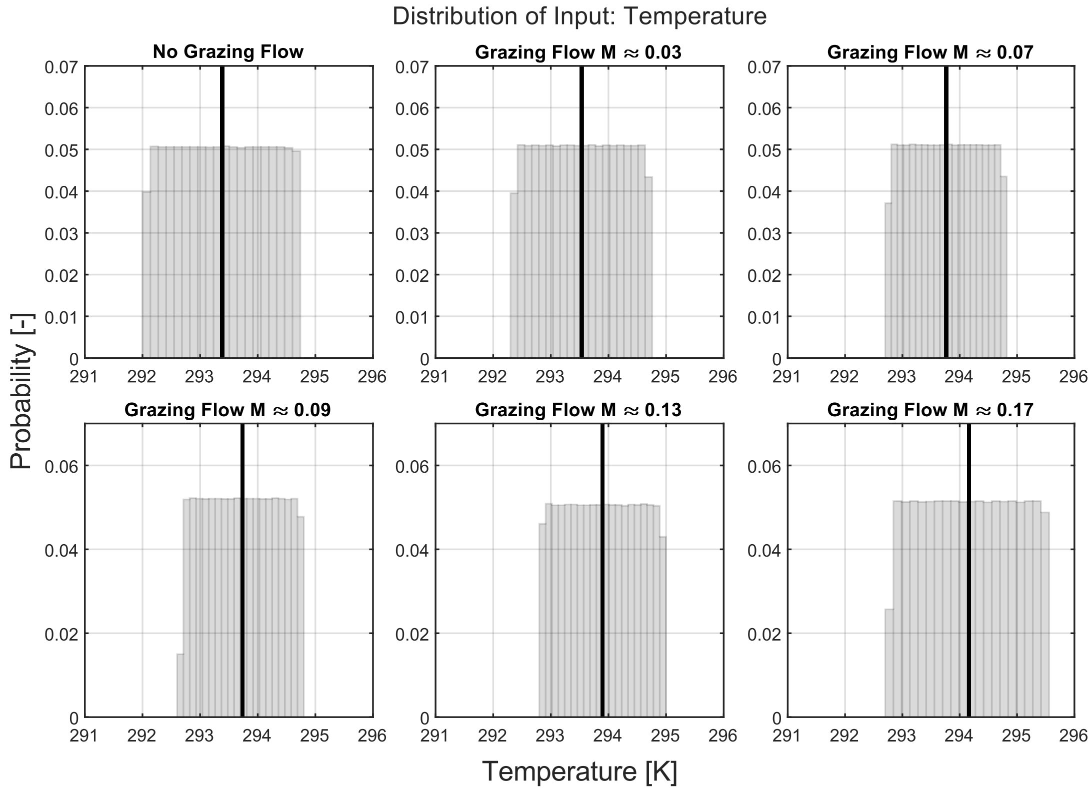

Figure 2 Uncertainty distribution of static temperature at different grazing flow speeds. Black lines : measured values; Shaded: probability distribution of input to Eq. (3)

3.2 Monte-Carlo Simulation

Monte-Carlo simulation is based on defining a linear data reduction system (F), which includes a set of equations describing the resistance (R) in terms of the inputs ($T, U, p,$ and s):

$$R = \mathrm{F}(T, U, p, s) \qquad (3)$$

Using the distributed inputs, the uncertainty in the output is determined, and can be described using the 95% confidence interval (CI). It is calculated as $\mu_{\mathrm{MC}} \pm 2\sigma_{\mathrm{MC}}$, where μ_{MC} is the mean of the output, and σ_{MC} is the standard deviation of its distribution.

4. Results and Discussion

The 95% CI of the resistance under excitation from three-different directions and different grazing flow speeds is as shown in Figures 3 to 5.

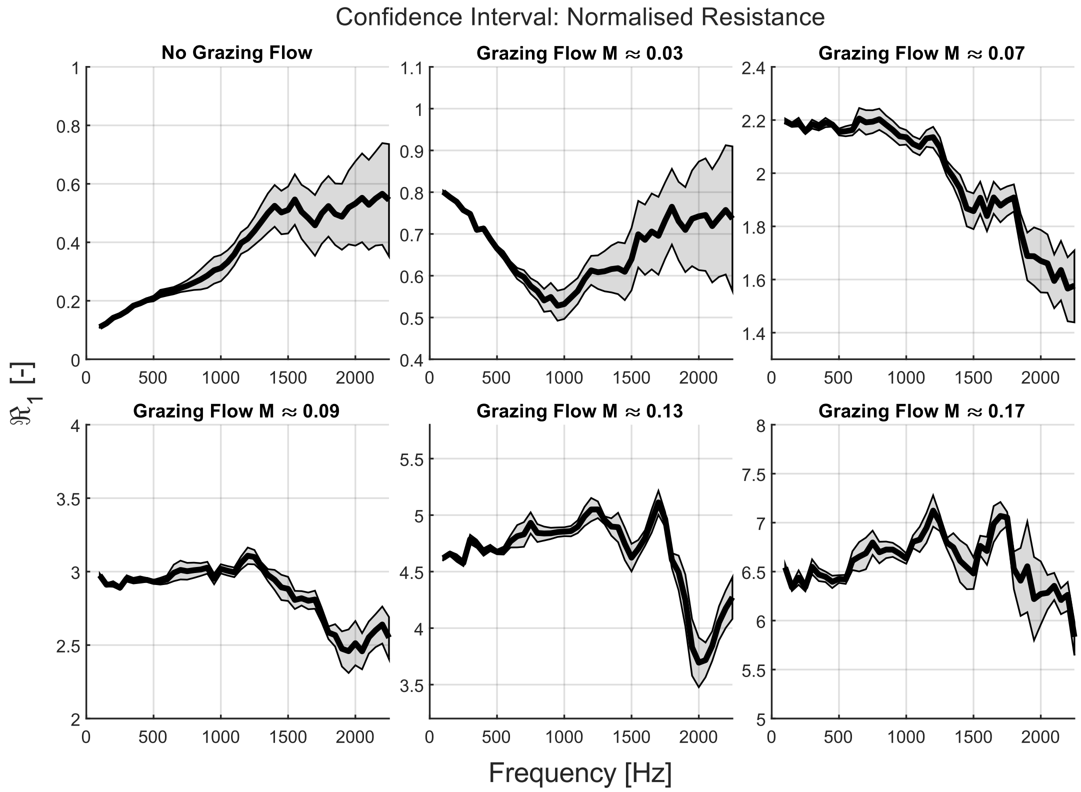

Figure 3 95% CI of normalised resistance under excitation from duct-1. Solid line: Measured value; Dotted line: mean of output of Monte-Carlo simulation; Shaded: confidence interval.

For a flow speed based Strouhal number > 0.7, the nature of the resistance is mainly governed by the acoustic field [5]. This Strouhal number limit is at ≈ 850 Hz and ≈ 1750 Hz for grazing flow $M \approx 0.03$, and 0.07, respectively. The narrower CI for the resistance till the Strouhal number limit, and for resistance in presence of high-speed grazing flow suggests that the uncertainty in the resistance is weakly dependent on the grazing flow velocity.

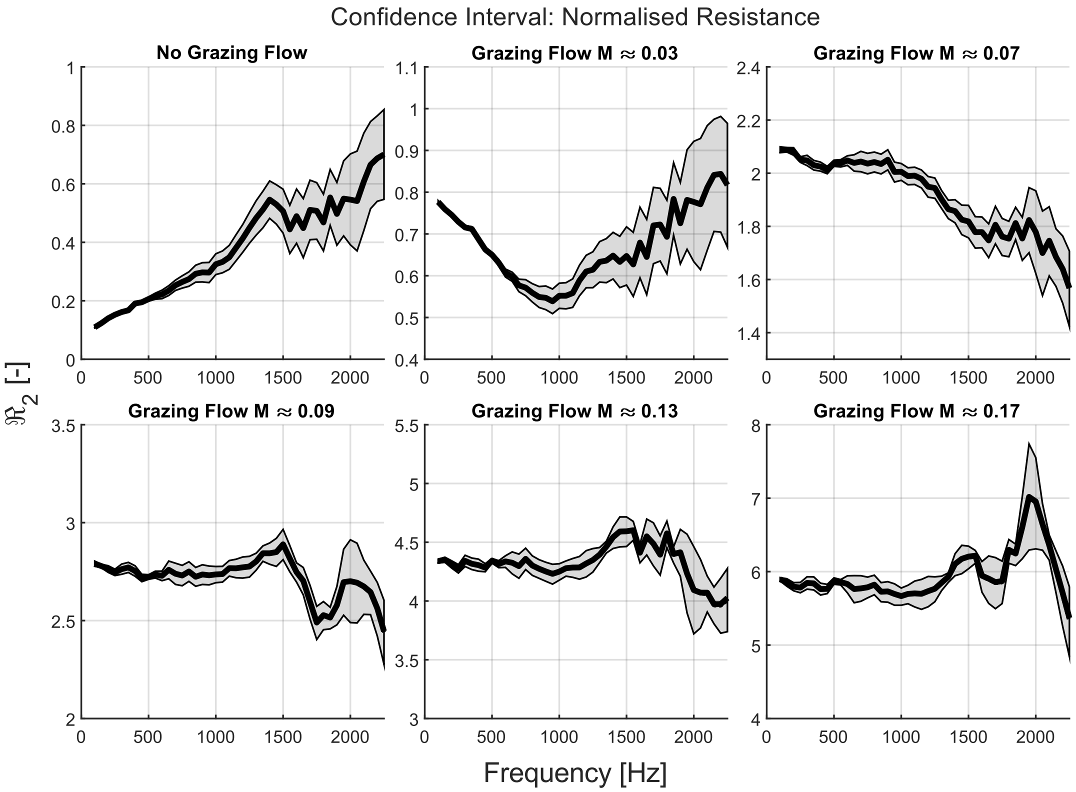

Figure 4 95% CI of normalised resistance under excitation from duct-2. Solid line: Measured value; Dotted line: mean of output of Monte-Carlo simulation; Shaded: confidence interval.

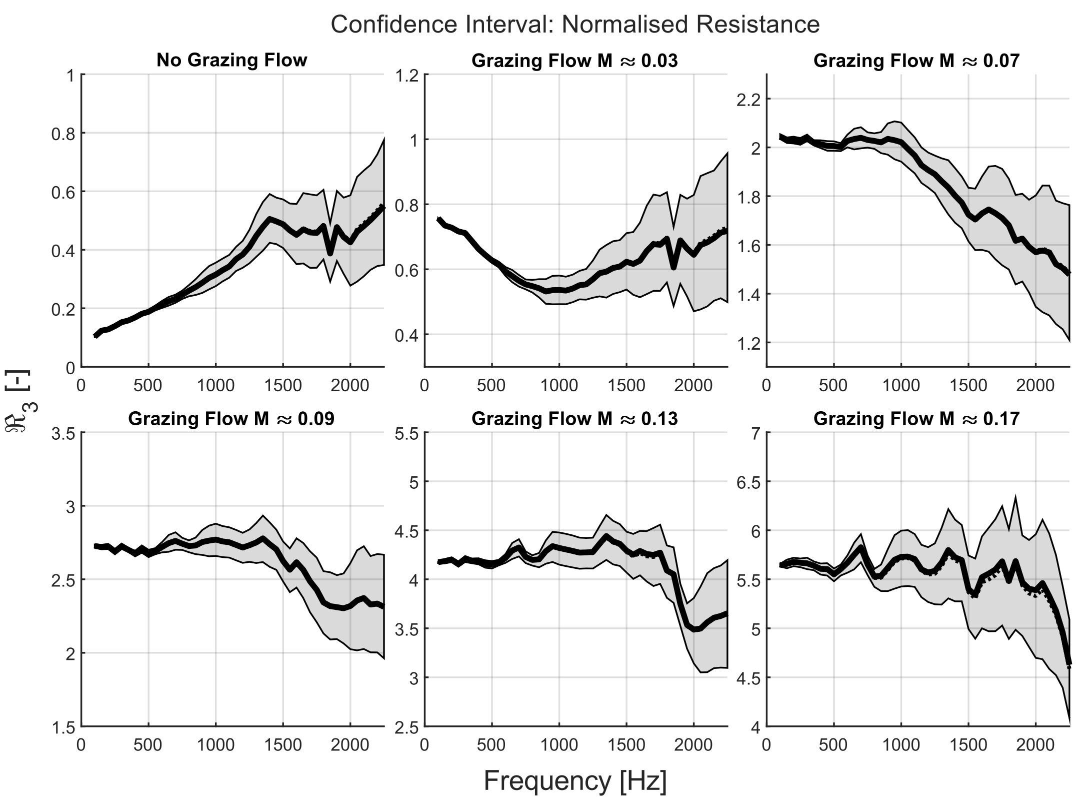

Figure 5 95% CI of normalised resistance under excitation from duct-3. Solid line: Measured value; Dotted line: mean of output of Monte-Carlo simulation; Shaded: confidence interval.

Further analysis of the uncertainty of the resistance on the uncertainty of input requires a global sensitivity analysis. Using the first order sensitivity indices, the quantification of the importance of each input factor, i.e., the sensitivity, can be calculated [12].

5. Conclusion

This study attempts to quantify the resulting effect of possible uncertainties in the inputs of the multi-microphone method. The factors considered are the uncertainty in the estimation of the in-duct temperature, the grazing flow speed, the acquired acoustic pressure signal, and the location of the microphones. The uncertainty range of the inputs as well as its distribution is explained. The effect of these uncertain inputs on the output, i.e., the normalised transfer resistance of a perforate sample is displayed. The calculation of the resistance is carried out using the three-port measurement technique. Using a Monte-Carlo simulation, the 95% confidence interval of the resistance under acoustic excitation from three-different directions and in presence of grazing flow is determined. A follow-up sensitivity analysis, to quantify of the effect of inputs on the resistance can be further studied.

REFERENCES

1 Bodén, H., Zhou, L., Cordioli, J., Medeiros, A. and Spillere, A., *On the effect of flow direction on impedance eduction results*, in *22nd AIAA Aeroacoustics Conference*. 2016.

2 Dean, P.D., *An In-Situ method of wall acoustic impedance measurements in flow ducts.* Journal of Sound and Vibration, 1974. **34**: p. 97-130.

3 Kooi, J.W. and Sarin, S.L., *An experimental study of the acoustic impedance of Helmholtz resonator arrays under a turbulent boundary layer*, in *7th AIAA Aeroacoustics Conference*. 1981.

4 Shah, S.A., Bodén, H., Boij, S. and D'elia, M.E., *Three-port Measurements for Determination of the Effect of Flow on the Acoustic Properties of Perforates*, in *AIAA AVIATION 2021 FORUM*. 2021: Virtual Event.

5 Shah, S.A. , *Experimental Investigation of the Acoustic Properties of Perfroate using Acoustic Three-Ports*. 2022, KTH Royal Institute of Technology: Stockholm.

6 Shah, S.A., Bodén, H. and Boij, S. *Study On the Effect of Operating Conditions on Acoustic Three-Port Measurements of Perforates in presence of Grazing Flow*. in *51st International Congress and Exposition on Noise Control Engineering*. 2022. Glasgow, UK.

7 Karlsson, M. and Åbom, M., *Aeroacoustics of T-junctions-an experimental investigation.* Journal of Sound and Vibration, 2010. **329**: p. 1793-1808.

8 Peerlings, L., *Assessing precision and accuracy in acoustic scattering matrix measurements*. 2017, KTH Royal Institute of Technology.

9 National, Instruments, *NI 9213 Datasheet*. 2022. p. https://www.ni.com/docs/en-US/bundle/ni-9213-specs/page/overview.html.

10 Swema, AB, *Swema 3000 Datasheet*. 2023. p. https://swema.com/wp-content/uploads/2022/11/swema-3000-product-sheet.pdf.

11 Sobol, I.M., *On the distribution of points in a cube and the approximate evaluation of integrals.* USSR Computational Mathematics and Mathematical Physics, 1967. **7**(4).

12 Saltelli, A., Ratto, M., Andres, T., Campolongo,F., Cariboni, J., Gateli, D., Saisana, M., and Tarantola,S. , *Global Sensitivity Analysis. The Primer*. 2008: John Wiley & Sons, Ltd.